Technical Notes

Measurement of Individual Particle Velocities in a Simulated Rocket Exhaust

R. D. FULMER* AND D. P. WIRTZ†
U. S. Naval Ordnance Test Station, China Lake, Calif.

Introduction

THE effects of particles in the exhausts of rocket motors have received considerable attention in the past few years. Numerous analytical studies have been conducted into the flow degradations associated with the velocity lag of such particles. Successful experimental measurements of the actual lag of the particle are needed, however, to confirm the theories and provide information needed for calculations.

To aid in studies of gas-particle flows, a technique was developed to measure the velocity of individual particles. The goal of the project was to measure the velocity of particles as small as 2 or 3μ, traveling at speeds up to 5000 fps. The gas velocities used in the experiments reported here limited particle velocities to around 2600 fps.

A series of controlled tests were run to check out the new technique. From these tests, data were obtained on the velocity lag of particles as a function of the particle diameter.

Measurement Technique

A study was conducted on possible approaches for measuring the velocity of small particles. Photographic techniques appeared to be the most promising.[1] One technique was chosen for development, in which two precisely timed exposures were taken of the particles. Knowing the duration between exposures and the distance between the streak-type images obtained on the film, it was possible to determine the velocity of the particle.

Light source

A krypton-gas light bomb was the key component in the measuring system. It was used both to front-light the small particles and shutter the event. In such light sources, an extremely intense light emission is obtained as the shock wave from an explosive charge travels through a volume containing one of the noble gases. The duration of the flash can be controlled by varying the length of gas through which the shock propagates.

For the measurements reported here, two light pulses were produced by passing a single shock through two bodies of emitting gas placed in tandem. One-half-inch tetryl pellets were used for the explosive charges. The time duration between the start of each pulse was determined precisely and found to be quite reproducible (3.14-μsec duration with a standard deviation of 0.04 μsec). The first flash was of a much longer duration than the second, which aided in identifying the streaks traced by particles on the film. The rise time of the light flashes was small in comparison to the time between flashes. Thus, the starts of each of the two streaks were well defined and made good points from which to measure. The gas cavities were $\frac{1}{2}$ in. in diameter. The light emitted from the cavity was focused down to a circle $\frac{3}{8}$ in. in diameter by a set of condensing lenses. The explosive charge, gas gaps, and accessory parts were enclosed within a metal housing to protect surrounding instruments from small fragments (Fig. 1).

Camera-Recording system

A plate camera equipped with a Wollensak $f/1.9$ lens was used to record the particle images. The camera was modified for 10X magnification. The reason for this was twofold: 1) it was necessary to magnify in order to pick up the small particles, and 2) the magnification allowed a measurable streak length on the film although holding the actual distance traveled by the particles to a minimum. Since the light source was used to shutter the event, special camera shuttering was not needed. Tests were run in the dark with the camera shutter open during the entire event.

Polaroid Pola Scope type 410 land film with an equivalent American Standards Association (ASA) rating of 10,000 was used in most of the tests. This film was used because of the ultrahigh film speed needed in the experiment and the ease and speed of photo processing.

Flow simulation

Particle-gas flows were produced using helium gas (total temperature of about 540°R) in a two-dimensional glass-walled nozzle chamber unit (Fig. 1). A sonic nozzle (no divergent section) having a 7°-half-angle convergent section was used. Aluminum powder was vibrated through a cloth filter bag to eliminate clumping. It was then picked up by a second helium stream and injected into the plenum chamber, upstream of the nozzle section.

Preliminary tests were run with the flow system to determine the total chamber pressure at which the flow just becomes sonic. Under these conditions the exit pressure just equaled ambient pressure, and a small region existed immediately downstream of the nozzle where the gas velocity (about 2900 fps) remained nearly constant. All of the particle velocity measurements were taken in this region.[1]

Attempts were made to obtain commercially available powders with small particle-size distributions. No suitable powders were found; therefore, commercial powders were processed (screened) to obtain powder fractions with smaller distributions. Size distribution data were obtained by taking photomicrographs of particle samples obtained from the

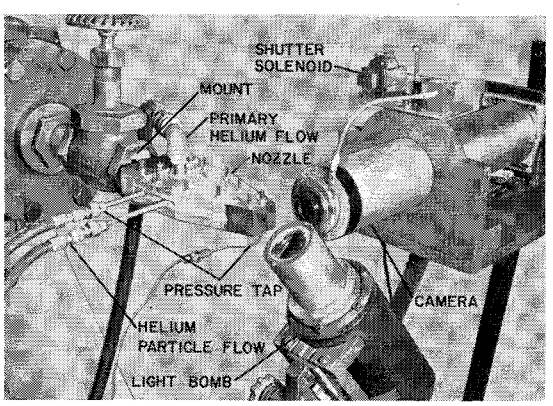

Fig. 1 Arrangement of flow, light bomb, and camera systems used in particle velocity measurement studies.

Presented as Preprint 65-11 at the AIAA 2nd Aerospace Sciences Meeting, New York, N. Y., January 25–27, 1965; revision received April 5, 1965.

* Research Aerospace Engineer, Propulsion Development Department. Member AIAA.

† Research Aerospace Engineer, Propulsion Development Department.

nozzle flow and counting the number of particles in given size ranges. The smallest fraction ranged from about 0 to 10μ, the largest from about 30 to 45 μ. The other two ran from about 15 to 30 μ.

Test setup

The camera, light bomb, and flow systems were integrated as shown in Fig. 1. Tests were run remotely and were quite simple in operation. After the light bomb was loaded and the camera set, the lights were turned off in the firing bay. The particle generator (vibrator) was actuated, both helium flows were started, and the camera shutter opened. The light bomb was fired, and the system was shut down. Further detailed information on the components and test setup can be found in Ref. 1.

Photographic results

Figure 2 shows a typical picture obtained with the technique. A large-diameter aluminum powder (30 to 40 μ) was used in this particular case to show better some of the characteristic traces. It should be observed that, on the good traces, there is a long streak followed by a much shorter one. In many cases this resembles a horizontal exclamation point and is the result of the two flashes.

The width of the streak increases with particle size. This results from two causes: 1) a larger particle has a greater reflecting surface, and 2) the larger particle has a longer effective exposure time (which results in overexposure of the film and, in turn, halation). This latter effect makes the particles appear much larger than they really are.

It should be noted also that not all of the streaks begin cleanly, and in many cases the second, shorter trace may be missing completely. This results primarily from the very shallow depth of field caused by the large lens opening used, the 10X magnification, and the very small allowable circle of confusion. Thus, small particle tracing trajectories at angles as shallow as 1° to the plane of interest can go in and out of focus during the time it takes to traverse one streak length. This actually is a distinct benefit to the experiment. Errors resulting from velocity components at right angles to the measurement plane are nearly eliminated.

Experiments

During the program, 45 tests were run in which particle pictures were taken. Thirty-five of these tests were made in the process of developing the technique. In these early tests, various unscreened powders were used, and conditions in the flow system were not carefully governed. The remaining 10 tests were run under controlled flow conditions with the sieved powder fractions. From the 10 photographs, a total of 98 particle velocity measurements was made.

The distance between the start of the streaks in each pair was measured with a 6X comparator to an accuracy of about 0.01 in. The magnification and camera field of view were obtained by taking a picture of a millimeter grid, which could be attached to the end of the nozzle.

Knowing the measured distance s between streaks, the magnification m of the lens system, and the time duration t between the onset of the two streaks, the particle velocity is calculated easily from $v = s/mt$. In all of the 10 cases, the magnification was 9.51, and the time duration was 3.14 μsec between flashes.

Results

Approximate velocity distribution was obtained for each powder fraction. The smallest particles, as would be expected, exhibited the higher velocities and the least velocity lags. The highest velocity measured was 2600 fps; this was for a 2- to 3-μ particle. From here, the measurements extended down to around 700 fps for particles in the 40- to 45-μ range.

The velocity distributions then were compared with the size distributions for the different powders. A range of possible particle sizes corresponding to selected values of particle velocity was obtained by noting the end points and the mean values of both distribution curves. This process was performed independently by both authors to obtain two sets of data that could be compared. The simplified approach used to correlate the data was necessary in view of the limited number of particle velocity measurements. The resulting velocity figures were normalized by dividing the particle velocity by the gas velocity (2900 fps), and the resulting ratio was plotted against particle size (Fig. 3). Because of the relatively small number of particles in the gas flow, it was assumed that the gas velocity was unaffected by the presence of the particles. The width of the horizontal lines indicates the uncertainty in the data. A curve has been drawn through the data to aid the reader.

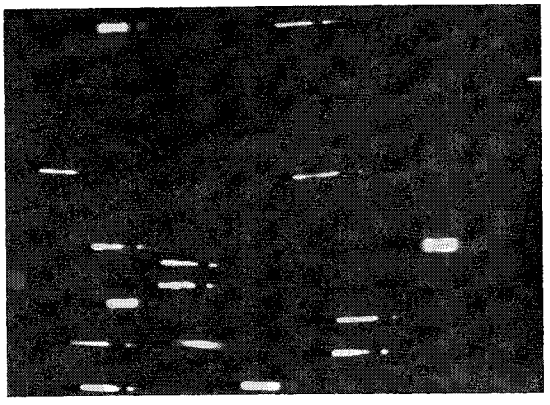

Fig. 2 Photograph of 30- to 40-μ aluminum particles in helium flow.

For comparison, theoretical data based on the test conditions and nozzle geometry also were plotted on the graph. The theoretical values were calculated, using one-dimensional particle-flow equations and assuming a constant particle-to-gas velocity ratio.[2] The assumption simplifies the solution of the equations. The results of the calculations usually agree quite well in the throat region with the generalized one-dimensional calculations.

The trends of the experimental and theoretical curves agree fairly well. The velocity lag, however, is not as great as predicted by the theory. The results indicate that a further extension and refinement of the work reported here would be desirable. A comparison of the data with two-dimensional theory would also be of interest.

Although the highest velocity recorded was only 2600 fps, the technique should be capable of measuring higher particle velocities. In the case reported here, the carrier gas velocity limited available particle velocities. With further optimiza-

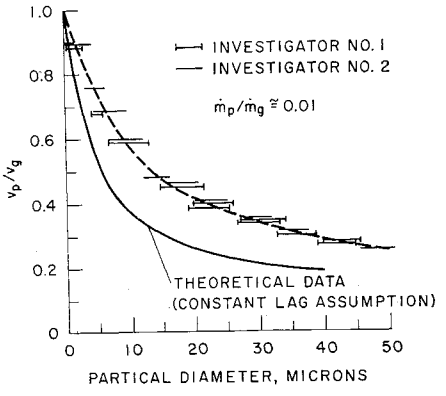

Fig. 3 Particle velocity normalized with the gas velocity (2900 fps) as a function of particle size for experimental and theoretical data.

tion of the system, it should be possible to record particles traveling at the original velocity goal, 5000 fps.

References

[1] Fulmer, R. D. and Wirtz, D. P., "Measurement of particle velocities in supersonic gas streams," U. S. Naval Ordnance Test Station, Bureau of Naval Weapons Rept. 8505, NOTS TP 3487 (December 1964).

[2] Crowe, C. T., Wolfolk, R. W., Dunlap, R., Woldridge, C.E., and Willoughby, P. G., "Dynamics of two-phase flow, twelfth quarterly technical progress report for Period 1 February 1964 through April 1964," United Technology Center Rept. 2005-QT12, pp. 38–44 (May 28, 1964).

A Regularized Approach to Universal Orbit Variables

EDWARD T. PITKIN*
University of Connecticut, Storrs, Conn.

Nomenclature

$\hat{C}$ = universal variable, Eq. (13)
D = $r\dot{r}/\nu$
E, F = eccentric anomaly, elliptic and hyperbolic
$\mathfrak{F}, \mathfrak{G}$ = representation coefficients, Eqs. (24) and (30)
$\hat{M}$ = universal time variable, Eq. (14)
$\mathbf{R}$ = $\mathbf{r}\,r^{-1/2}$
$\hat{S}, \hat{U}$ = universal variables, Eqs. (13) and (15)
T = time of pericenter passage
$\hat{X}$ = universal eccentric anomaly, Eq. (4)
a = semimajor axis
e = eccentricity and base of natural logarithms
f, g = representation coefficients, Eq. (26)
h = Eq. (34)
i = orbit inclination angle
$\mathbf{r}, r$ = position vector, radius
$\dot{\mathbf{r}}, \dot{r}$ = velocity and radial component
$\mathbf{r}', r'$ = transformed velocity and radial component
v = true anomaly
α = energy constant, $-1/a$
β = $(\alpha)^{1/2}\hat{X}$
ν = gravitational constant, Eq. (1)
τ = time variable
ω = argument of pericenter
Ω = longitude of ascending node

Superscripts and subscripts

$(\dot{\ })$ = $d(\ )/d\tau$
$(\ )'$ = $d(\ )d\hat{X}$
0 = evaluated at epoch τ_0

I. Introduction

THE recent introduction of rocket propulsors for space flight has presented possibilities of encountering orbits whose character changes significantly during the time of interest. For instance, a low-acceleration escape trajectory might begin in a nearly circular orbit and terminate on a hyperbolic path. This aspect, as well as the nearly universal use today of electronic computers for orbit computation and the attendant desire to simplify programing, motivate one to employ a formulation free from possibilities of indeterminateness, no matter what geometric form the orbit takes, be it elliptic, parabolic, hyperbolic, or possibly a circular or rectilinear limit.

In 1947 Stumpff[1] found a formulation free of indeterminateness by algebraic rearrangement of the classical orbit formulas. Herrick[2] more recently introduced a related but algebraically simpler formulation, again by an heuristic rearrangement of classical forms so that elliptic, parabolic, and hyperbolic cases could be expressed in terms of a generalized eccentric anomaly $\hat{X}$, e.g., $\hat{X} = (a)^{1/2}(E - E_0)$ in elliptic orbits. In both methods the classical elements a, e, i, Ω, ω, and T are replaced by the six components of position and velocity at some reference epoch $\mathbf{r}_0 = \mathbf{r}(\tau_0)$, $\dot{\mathbf{r}}_0 = \dot{\mathbf{r}}(\tau_0)$. These vectors have significance in a two-body orbit of any geometric shape and, in themselves, introduce no indeterminateness, as contrasted to the Euler angles i, Ω, ω.

The purpose here is to derive Herrick's universal expressions via regularization and integration of the two-body differential equations of motion and thereby place the universal variables on a somewhat more formal mathematical foundation. As a result of this approach, an alternate set of "conditioned" elements, which remain bounded even at the origin arises naturally. Because the universal formulation is developed primarily for numerical work with electronic computers, the proper computational sequences so important to maintain good accuracy and high speed also will be discussed.

II. Regularizing Transformation

The vector differential equation for the relative motion of a pair of mutually attracting mass points with inverse square gravitational fields is

$$\ddot{\mathbf{r}} = -\nu^2\mathbf{r}/r^3 \tag{1}$$

where ν is the square root of the usual gravitational constant μ. A first integral, the energy or Via Viva, is obtained after taking the inner product with $\dot{\mathbf{r}}$

$$\dot{\mathbf{r}}\cdot\dot{\mathbf{r}}/\nu^2 = 2/r + \alpha \tag{2}$$

where α, the integration constant, may be determined by this equation evaluated at a particular epoch τ_0.

Inspection of the equation of motion (1) reveals a second-order singularity at $r = 0$. A solution valid in the neighborhood of this singularity will be possible only if the point can be regularized by a change of variables so that the singularity becomes a regular point in the transformed coordinates. The regularizing transformation that will be used here is that introduced by Sundman[3] in connection with the three-body problem.† It may be expressed as

$$d(\ )/d\hat{X} = (r/\nu)\,d(\ )/d\tau \tag{3}$$

or in the integrated form

$$\hat{M} \triangleq \nu(\tau - \tau_0) = \int_0^{\hat{X}} r\,d\hat{X} \tag{4}$$

where $\hat{X}$ is taken to be zero at τ_0.

Application of (3) to (1) then gives the transformed equation of motion regular at $r = 0$ where the prime denotes differentiation with respect to $\hat{X}$

$$\mathbf{r}'' - r'\mathbf{r}'/r + \mathbf{r}/r = 0 \tag{5}$$

The magnitude of the third term is unity, so it gives no difficulty. To show that the second term also remains

Received December 15, 1964; revision received April 5, 1965. Condensed from portions of the author's Ph.D. Dissertation.[4] This work was supported partially by the NASA Predoctoral Trainee program.

* Associate Professor of Aerospace Engineering; formerly NASA Predoctoral Trainee, University of California at Los Angeles, Los Angeles, Calif. Associate Fellow Member AIAA.

† Sperling[6] also has used the Sundman transformation and the energy integral to obtain a different form of Eq. (5), whose solution leads to a set of related universal variables that are functions of β only, but which also require carrying powers of $\hat{X}$ separately. Battin[7] employs a still different version (also functions of β only). Both sets can be deduced from the variables treated here by carrying the first terms of Eqs. (32) separately, plus some algebraic rearrangement. The author wishes to express his thanks to the reviewer for calling his attention to Ref. 6